Bayesian Modeling of Spatiotemporal patterns of TB-HIV co-infection risk in Kenya

Verrah A Otiende (verrahodhiambo@gmail.com)
Pan African University https://orcid.org/0000-0001-6147-3547
Thomas N O Achia
University of the Witwatersrand Faculty of Health Sciences
Henry G Mwambi
University of KwaZulu-Natal

Research article

Keywords: Bayesian modeling, TB-HIV co-infection, co-epidemic burden, Kenya

Posted Date: October 22nd, 2019

DOI: https://doi.org/10.21203/rs.2.9411/v3

Version of Record: A version of this preprint was published on October 28th, 2019. See the published version at https://doi.org/10.1186/s12879-019-4540-z.

Bayesian Modeling of Spatiotemporal patterns of TB-HIV co-infection risk in Kenya

Verrah Otiende[1*], Thomas Achia[2], Henry Mwambi[3]

[*]Correspondence: otiende.verrah@students.jkuat.ac.ke; verrahodhiambo@gmail.com

Abstract

Background

Tuberculosis (TB) and Human Immunodeficiency Virus (HIV) diseases are globally acknowledged as public health challenges exhibiting adverse bidirectional relations due to the co-epidemic overlap. To understand the co-infection burden we used case notification data to generate spatiotemporal maps to describe risk patterns for further epidemiologic investigations. These model maps are relevant for geographically targeting interventions towards suppressing co-infection

Methods

We analyzed the TB and TB-HIV case notification data from the Kenya national TB control program aggregated for forty-seven counties over a seven-year period (2012 – 2018). Using the Integrated Nested Laplace Approach (INLA), we modeled the risk of TB-HIV co-infection. Six competing models with varying space-time formulations were compared to determine the best fit model. We assessed the space-time patterns of coinfection risk by mapping the posterior marginal from the best fit model.

Results

Of the total 608312 TB case notifications, 194129 were HIV co-infected. The proportion of TB-HIV co-infection was higher in female (39.7%) than to male (27.0%). A significant share of the co-infection was among adults aged 35 to 44 years (46.7%) and 45 to 54 years (42.1%). Based on the Bayesian Defiance Information (DIC) and the effective number of parameters (pD) comparisons, the spatiotemporal model 3b

was the best in explaining the geographical variations in TB-HIV coinfection. The model results suggested that the risk of TB-HIV coinfection was influenced by infrastructure index (5.75, Credible Interval (Cr.I) = (1.65, 19.89) and gender ratio ($5.81e^{-04}$, Cr.I = ($1.06e^{-04}$, $3.18e^{-03}$)). The lowest and highest temporal risks were in the years 2016 at 0.9 and 2012 at 1.07 respectively. The spatial pattern presented increased co-infection risk in various counties. For the spatiotemporal interaction, few counties had a probability of risk greater than 1 that varied in different years.

Conclusions

TB-HIV co-epidemic in Kenya is at a critical point portending a dual endemic challenge for many years to come. Integration of care for both TB and HIV using a single facility and single health provider in each county will enable proper monitoring of the co-infection trends and subsequently significant reduction of HIV burden amongst TB patients and TB burden amongst HIV patients

Keywords

Bayesian modeling, TB-HIV co-infection, co-epidemic burden, Kenya

Background

Tuberculosis (TB) and Human Immunodeficiency Virus (HIV) diseases have a co-epidemic relation such that the chronic immune prompt arising from TB disease hastens HIV disease advancement (1,2). Both the TB and HIV pathogens interact collectively, accelerating the progress of illness thereby increasing the chances of death (3). Globally, TB and HIV exhibit an adverse bidirectional interaction because of the co-epidemic overlap. The risk of TB infection developing into TB disease is between 16-27 times higher in HIV infected persons (4). TB can occur both in the early stages and through all stages of HIV infection although the risk intensifies soon after infection with HIV (5).

Under the same degree of exposure, there exists no irrefutable evidence that HIV positive persons are more likely to acquire TB infection than HIV negative persons (6). However, the risk of rapid progression once TB infection occurs is greater among persons living with HIV infection (7,8). The lifetime risk for HIV

47 negative individuals to develop active TB from latent TB is about 5% to 10%, whereas, for persons living
48 with HIV, the same percentage holds but annually opposed to lifetime (9). Studies by (10) and (11) in
49 various outbreak settings confirms that HIV co-infection does intensify the progression of latent TB to
50 active TB disease. The diagnosis of TB in the HIV epidemic remains extremely challenging because of the
51 difficulty in differentiating between reactivation and recent infections (12). The risk of infection or
52 reinfection is dependent on the source case numbers in various congregate settings including households
53 and health-care facilities (5)

54 The disparity for TB infections between persons with and without HIV infection remains a global concern
55 especially because of the high incidence rate among HIV infected persons (13). A study by (14) observed
56 that the prevalence of HIV infections for persons reporting prior TB disease was 33.2% compared to 5.1%
57 in persons without prior TB. Another study by (13) confirmed that TB disease incidence among HIV
58 infected persons was still eight times higher than in persons without HIV. In the year 2015, the global
59 estimation of TB disease was 10.4 million of which 11% were HIV positive (15). Approximately 60% of
60 the TB/HIV co-infected patients received neither diagnosis nor treatment leading to 390,000 TB related
61 deaths (16).

62 Globally, sub-Saharan Africa accounts for the largest percentage of the dual epidemic with co-morbidity
63 from TB-HIV remaining a critical public health challenge (14). In essence, more people die from TB than
64 HIV associated infections (17). In 2016 alone, the SSA region accounted for an estimated 86% of HIV-
65 linked TB deaths (18). Kenya is one of the countries in SSA severely hit by the dual epidemic and appears
66 among the WHO high TB and TB-HIV burden countries ranking 13 out of the 22 countries globally (19,20).
67 The impact of TB-HIV co-infection in Kenya is evident mainly because of the complications in diagnosis
68 and management. Equally, the HIV surveillance on TB patients and the TB surveillance on HIV patients in
69 Kenya relies primarily on the self-reported cases from health facilities as a surrogate measure of the actual
70 co-endemic. The two surveillance systems are not integrated making it a challenge to profile the actual co-
71 infection burden. Therefore, the feasibility of using case notifications instead of population-based studies
72 to capture the valid spatiotemporal co-infection incidence estimates of the co-epidemic is unknown

Against this background, we investigate the geographical variation and co-infection burden using the case notification data for a 7-year period and characterize the areas with unusually high relative risks. We utilize the space-time disease mapping models which allow for the concurrent study of persistent and unusual co-infection trends, thus offering additional benefits over purely spatial disease mapping models (21,22). These model-maps describe new exposure hypotheses that warrant further epidemiologic investigations in areas with unusual case notification levels and ultimately inform relevant geographically based interventions and resource allocation towards suppressing further infections.

Methods

Data Sources

We conducted this study through extensive analysis of TB case notification data from the Kenya national TB control program database. The database is an elaborate and robust surveillance system that captures case notification data from the health facilities in every county and updates the records on the national grid. For the process of data capture into the surveillance system, the National TB program adapted both the recording and reporting tools from WHO. The WHO recommends systematic screening for HIV among TB patients; our dataset captures the HIV status of all the TB case notifications. We analyze the data aggregated at the county level.

Model Description

For the county s in the year t, we modelled the TB-HIV cases notification y_{st} as

$$y_{st} \sim Poisson(\lambda_{st})$$

We assumed our count data follows the Poisson distribution where the log of the relative risks was the focus of modeling. We defined the mean λ_{st} in terms of the unknown relative risk and expected number of co-infection cases i.e. $\lambda_{st} = \rho_{st} E_{st}$.

We defined the population at risk of TB-HIV co-infection are the TB cases. We computed the expected counts of co-infection cases E_{st} per county per year. These counts represent the number of cases one would

97 expect if the population of county s has a similar behavior to the standard population. Our statistical
98 consideration for the standard population N was the average of the pooled TB cases, i.e. $N = \frac{P}{Y}$, where P is
99 the total number of TB cases at risk of co-infection and Y is the number of years, which is seven for this
100 study. We calculated the crude rate as $R_{st} = \frac{\sum X_{st}}{P_{st}}$, where $\sum X_{st}$ and P_{st} are the number of co-infection cases
101 and number of TB cases in county s, year t respectively. We then multiplied the crude rate by the standard
102 population to obtain the expected number of co-infection cases

103 $$E_{st} = R_{st} \times N$$

104 We expressed the linear predictor on the logarithmic scale, $\eta_{st} = log\ (\rho_{st})$ which is the recommended
105 invertible link function for the Poisson family of distributions. We compared the spatiotemporal disease
106 models discussed by (23). The models differed in their formulation of the space-time structure and the
107 inclusion or not of the covariates. Model 1a applied the classical parametric formulation of (24) on the
108 linear predictor, which we expressed as

$$\eta_{st} = \alpha + \upsilon_s + \nu_s + (\rho + \delta_s) \times Z_t \quad (1a)$$

109 The formulation included the spatially structured (υ_s) and unstructured (ν_s) random effects, the global
110 linear time trend effect $(\rho \times Z_t)$. The term $\delta_s \times Z_t$ is the interaction term between space and time defining
111 the difference between ρ and the area specific time trend. It is referred to as the differential trend of the s^{th}
112 area (23,24). The term Z_t is a vector of temporal weights and the intercept α quantifies the average co-
113 infection rate in all the 47 counties. Each spatial unit has its own time trend with a spatial intercept $(\alpha +$
114 $\upsilon_s + \nu_s)$ and a slope $(\rho + \delta_s)$. This model assumes a linear time trend in each spatial unit. We estimated
115 the parameters $\theta = \{\alpha, \rho, \nu, \upsilon, \delta\}$ and the hyper-parameters $\psi = \{\tau_\nu, \tau_\upsilon, \tau_\delta\}$.

116 The model 1b included the covariates to the model 1a thereby estimating $\theta = \{\alpha, \beta, \rho, \nu, \upsilon, \delta\}$ and $\psi =$
117 $\{\tau_\nu, \tau_\upsilon, \tau_\delta\}$. The model expression was

$$\eta_{st} = \alpha + \sum \boldsymbol{\beta_i x_i} + \upsilon_s + \nu_s + (\rho + \delta_s) \times Z_t \quad (1b)$$

118 The model 2a used the dynamic non-parametric formulation on the linear predictor

$$\eta_{st} = \alpha + \upsilon_s + \nu_s + \gamma_t + \phi_t \quad (2a)$$

The terms α, υ_s and ν_s are similar to the formulation in the first model, additionally, the terms γ_t and ϕ_t represents the temporally structured and unstructured random effect respectively. The model assumes a non-parametric time trend. In this formulation, $\theta = \{\alpha, \nu, \upsilon, \gamma, \phi\}$ and $\psi = \{\tau_\nu, \tau_\upsilon, \tau_\gamma, \tau_\phi\}$.

The model 2b incorporated the covariates to the model 2a to estimate $\theta = \{\alpha, \beta, \nu, \upsilon, \gamma, \phi\}$ and $\psi = \{\tau_\nu, \tau_\upsilon, \tau_\gamma, \tau_\phi\}$. We expressed model 2f as

$$\eta_{st} = \alpha + \sum \boldsymbol{\beta_i x_i} + \upsilon_s + \nu_s + \gamma_t + \phi_t \quad (2b)$$

Our model 3a expanded the model 2a by allowing a space-time interaction to explain for the difference in the time trend of TB-HIV coinfection for the diverse counties.

$$\eta_{st} = \alpha + \upsilon_s + \nu_s + \gamma_t + \phi_t + \delta_{st} \quad (3a)$$

For this model, $\theta = \{\alpha, \nu, \upsilon, \gamma, \phi, \delta\}$ and $\psi = \{\tau_\nu, \tau_\upsilon, \tau_\gamma, \tau_\phi, \tau_\delta\}$. We defined δ_{st} as the interaction between ν_s and ϕ_t consequently assuming no interaction between υ_s and γ_t therefore $\delta_{st} \sim N(0, \tau_\delta)$.

The final model 3b incorporated the covariates to the model 3a to estimate $\theta = \{\alpha, \beta, \nu, \upsilon, \gamma, \phi, \delta\}$ and $\psi = \{\tau_\nu, \tau_\upsilon, \tau_\gamma, \tau_\phi, \tau_\delta\}$. We formulated the model as

$$\eta_{st} = \alpha + \sum \boldsymbol{\beta_i x_i} + \upsilon_s + \nu_s + \gamma_t + \phi_t + \delta_{st} \quad (3b)$$

To assess the performance of these six models, we used the DIC taking into consideration the complexity of the models. We selected the model with the lowest DIC as the best-fit model

Baseline predictor variables

The set of baseline predictors were poverty index, infrastructure index, health index, education index, gender ratio, dependency ratio, and Gini coefficient. The measures of these predictors were obtained from (25) and (26). These predictors are standard indices used to establish the comparative level of development of different counties in Kenya. The computation of these indices are further elaborated in the reports from

(25) and (26). All these predictor variables were fitted in the models 1b, 2b and 3b but only the significant ones were considered in the discussion.

The poverty index provides a measure on the inadequate consumption of basic services and fundamental rights. In other words, it estimates the disparities in resource expenditures for each county. The infrastructure index captures access to natural resources, economic growth and innovative planning. The health index measures access to medical services, adequate medical work force and improved medical productivity. The education index captures the literacy attainment, completion and dropout rate. The gender inequality index reflects the bias in reproductive health, empowerment and labor market between men and women. The dependency ratio gives an indication on the burden of the working population and government to support the non-working population who are either too young or too old. The Gini coefficient compares the distribution of income in the entire population of any given county. It is based on the Lorenz curve and varies between 0 (complete equality) and 1 (complete inequality).

Statistical Analysis

For the demographic characterization of the case notifications, we compared the summaries of TB cases with and without HIV infections. We stratified the data based on HIV status and performed the chi-square test to determine the association between HIV status and each of the demographic variables TB-type, age, gender, and patient type. All the p-values were two-tailed with values less than 0.05 considered being statistically significant. The TB type classification was either pulmonary TB or extra-pulmonary TB. Pulmonary TB referring to a patient with TB disease involving the lung parenchyma whereas the extra-pulmonary TB involves any organ other than the lungs. For the patient type, we had five categories; the first was the default category for patients who defaulted the TB therapy then experienced recurrence. The second was the failed category for patients previously diagnosed with TB but never took on the therapy. The third category was for newly diagnosed patients without previous TB diagnosis or therapy. The relapse case was the fourth category whereby patients were previously diagnosed, treated of TB and completed the TB therapy but experienced a recurrence. The fifth and final category were the cases transferred in from other health facilities to continue with the therapy.

Using the Integrated Nested Laplace Approach (INLA), we fitted the case notification data to our spatiotemporal disease models to determine the best fit. We assessed the nature of the response variables on our baseline predictors. We specified the Besag-York-Mollie (BYM) prior on υ_s using the intrinsic conditional autoregressive structure (iCAR) $\upsilon_{s_i}|\ \upsilon_{s_i \neq s_j} \sim N\left(\frac{\sum_{j \epsilon N(s)}\ \upsilon_{s_j}}{\#N(s)}, \frac{\sigma_\upsilon^2}{\#N(s)}\right)$ where $\#N(s)$ is the number of neighbors sharing boundaries with the county s_i. The BYM model allows us to capture both the heterogeneity (variability) and clustering of diseases risk simultaneously. We then used the exchangeable prior on ν_s, that is $\nu_s \sim N(0, \sigma_\nu^2)$. We modelled γ_t using a random walk specified through the temporal adjacency structure, which is analogous to the spatially structured random effects specification as it borrows strength from adjacent time periods. The temporally unstructured random effect ϕ_t was modelled using the Gaussian exchangeable prior $\phi_t \sim N(0, \tau_\phi)$. We defined improper priors for the intercept and regression coefficients of the fixed effects as $\alpha \sim N(0,0)$ and $\beta \sim N(0, 0.001)$ respectively. For the distribution of the hyper-parameters, we assumed the default specifications of INLA whereby we assigned minimally informative priors on the log of the precision of both the structured and unstructured effects $\psi \sim (1, 0.0005)$.

Results

Demographic characterization of TB-HIV case notification in Kenya, 2012-2018

Of the total 608312 TB case notification for the period 2012-2018 included in the study, 194129 cases were HIV co-infected, 391030 cases were HIV uninfected and 23153 cases were unaware of their HIV status because either the HIV test was not done or they declined to be tested. The demographic characteristics of TB patients stratified by HIV status are in Table 1. The TB case notification decreased from 99586 (16.4%) in 2012 to 78318 (12.6%) in 2016 but increased to 85886 (14.1%) in 2017 and 83324 (13.7%) in 2018. Similarly, the co-infection cases decreased from 36135 (36.3%) in 2012 to 21896 (26.3%) in 2018. The chi-square test showed that HIV status was positively associated to age, time of case notification, type of TB, gender and TB patient type (p-value <0.01)

186 The male TB case notification exceeded the female but the proportion of TB-HIV co-infection was higher
187 in female cases (39.7%) as compared to male cases (27.0%). The temporal trend of co-infection risk was
188 consistently higher in women (Figure 1) whereas the spatial pattern was widespread in males compared to
189 the female. The counties with high co-infection burden for both male and female were Homabay, Siaya,
190 Kisumu, Migori and Busia counties (Figure 2). A significant share of the co-infection was among adults
191 between the ages 35 to 44 years (46.7%) and 45 to 54 years (42.1%). Patients aged below 25 years and
192 above 54 years registered a considerably lower co-infection risk over time (Figures 3). The spatial patterns
193 based on age-categories showed a widespread co-infection risk pattern for the ages 25-34 followed by 35-
194 44 years (Figure 4). These age categories and generally the most sexually active age ranges, which puts
195 them at higher risk of co-infection.

196 The proportion of extra-pulmonary TB cases co-infected with HIV (35.6%) also surpassed that of
197 pulmonary TB (31.2%). Looking at the patient types, the 194129 TB-HIV co-infection cases were
198 composed of 171115 (31.0%) new TB infections, 17174 (42.9%) TB relapse cases, 457 (29.5%) TB therapy
199 failure cases, 3336 (37.5%) defaulted cases and 2047 (30.9%) transferred in cases.

200 ## Model comparison

201 In Tables 2 and 3 we present the results of the six hierarchical models including the Deviance Information
202 Criterion (DIC), the effective number of parameters (pD) and the mean deviance ($\check{D}$). We compared the
203 spatiotemporal disease models discussed by (23), which differed in their formulation of the space-time
204 structure and the inclusion or not of the fixed effects. The values of pD penalizes the complexity of the
205 model and smaller values indicates a parsimonious model. For Poisson likelihoods, the pD should be
206 approximately equal to the number of observations (27); that is $47 \times 7 = 329$. Model 1a has the smaller
207 pD than the number of observations and the biggest DIC, indicating a clear lack of fit. Both criteria thus
208 point to the model 3b being the best fitting model. In this model, the infrastructure index ($5.75, \mathrm{Cr.I} =$
209 $(1.65, 19.89)$) and gender ratio ($5.81\mathrm{e}^{-04}, \mathrm{Cr.I} = (1.06\mathrm{e}^{-04}, 3.18\mathrm{e}^{-03})$) were significantly associated
210 with TB-HIV co-infection. In the remaining sections, we focus on presenting the results on the model 3b.

Temporal characteristics of TB-HIV co-infection epidemics

The temporal trend in TB-HIV co-infection relative risks from 2012 – 2018 are in Figure 5. The co-infection risk trend shows an initial steady decrease between 2012 and 2016 then a sharp increase in 2017 that slightly decreases in 2018. The lowest risk of 0.9 was in the year 2016 while the highest risk of 1.07 was in the year 2012.

Spatial patterns of TB-HIV co-infection epidemic

The spatial map in Figure 6 and relative risk plot in Figure 7 present the cumulative predicted values of TB-HIV coinfection risk over a 7-year period (2012 – 2018) per county. There were 12 counties out of the 47 with high co-infection risk evidenced by values greater than 1. Most of these high-risk counties were towards the further west of Kenya; Homabay County was leading followed by Siaya, Kisumu, Migori and Busia counties

Figure 8(a) shows the spatial pattern of the posterior mean for the country-specific relative risk ($\zeta_s = e^{(\xi_s = \upsilon_s + \nu_s)}$) of TB-HIV co-infection compared to the whole of Kenya while Figure 8(b) presents the measure of uncertainty associated with the posterior means ζ_s: $P(\zeta_s > 1|y)$. It is evident that there is an increased co-infection risk in a number of counties characterized by a spatial relative risk above one and a posterior probability of the relative risk above 0.8 indicating a high level of associated certainty.

Spatiotemporal trends of TB-HIV co-infection epidemics

The probability maps for the space-time interaction relative risk estimates greater than one, $\mathrm{P}\left(\mathrm{e}^{\delta_{\mathrm{st}}} > 1|\mathrm{y}\right)$, for the seven years are in Figure 9. These are the exceedance probabilities useful for assessing unusual elevation of coinfection risk over the 7-year period of study. In relation to TB-HIV co-infection the specification for the spatiotemporal interaction assumed that the residual coinfection patterns were not correlated for adjacent county-year. This is evident as our results showed only a few counties had a probability of the relative risk being greater than 1 and they varied in different years.

Discussion

The surveillance data from the National TB program gives deep insights on the TB-HIV co-epidemic. This study established that 96% of the TB case notifications had documented HIV test results, which is greater than the WHO's global estimate of 64% in 2017 and that of the African region (86%) (28). The significant upturn in the HIV screening practices for every TB case notifications in Kenya could be attributed to the commitment from the National TB program and the health professionals in communication and social mobilization for early diagnosis and therapy uptake. Similar observations were reported in Ghana (29) and Ethiopia (30). Globally, Kenya registered 8% TB decline rate per year from 2013 to 2017 amongst other high TB burden countries including the Russian Federation (13%), Ethiopia (12%), Sierra Leone (10%) and Viet Nam at 8% (28).

Our findings on the number of TB case notifications per year for the period 2012 to 2018 showed a steady reduction for the period 2012 – 2016 then a significant rise in 2017 and a slow decrease in 2018. The temporal trend of the coinfection relative risk for the entire country followed a similar pattern as the TB case notifications. From 2012 – 2016, there was a clear downward relative risk trend then a steep upward risk for the year 2017 – 2018. This could be because of either improvement in TB cases detection or surveillance biases due to spatial heterogeneity in the co-infection dynamics, an observation that is in accord with the conclusions of (31). To maintain the consistent TB decline rates, supplementary efforts to support TB-HIV collaborative activities towards reducing the burden of HIV in TB patients are critical.

The co-infection cases were higher in patients aged between 35 – 54 years with new cases of TB infection. Similarly, the co-infection risk was higher for the same age bracket, which implied that co-infection was more common in the sexually active age group. These findings were contrary to the findings by (32) and (29) who observed that high rates of TB-HIV co-infections were in younger patients (<15 years of age) but consistent to several other studies (30,33–36). The study also revealed that a larger proportion of the HIV co-infected cases had extra-pulmonary TB conforming to (37) and (34) who found that the risk of extra-pulmonary TB was higher in HIV co-infected cases majorly because of delayed diagnosis especially for the sputum smear-negative

In our study, the male TB cases significantly exceeded female cases. However, the risk of co-infection was consistently higher in females than in males for the period 2012 – 2018. The findings conform to a number of studies showing that females bear a disproportionate burden of TB-HIV co-infection in SSA (14,38–41). The larger TB case notification among the male could be because of the barriers the female encounter in seeking care for and diagnosis of TB or could reflect more complete registration for treatment by the male (42). In other studies by (34), the prevalence of co-infection was much higher among males in most countries in Sub-Saharan Africa whereas in all other countries there was no significant difference in the gender ratio. However, the case notification data alone are insufficient to determine whether the gender ratio reflect an excess in the co-infection burden among men or a disadvantage among women in seeking and accessing TB care.

Having proper infrastructure in place is the foundation for planning, delivering and evaluating public health services. The country infrastructure ranking in (26) showed counties with infrastructure index below the national average of 0.41 were classified as the most marginalized. In our study, it was evident that counties in the western region of Kenya, that is Homabay, Siaya, Kisumu, Migori, Busia, and Vihiga, have unresolved co-infection dynamics that is echoed by their infrastructure index. Their patterns of co-infection also reinforced the fact that counties with high HIV prevalence also post high TB disease burden (43,44) with exception of a few like Wajir, Lamu, Isiolo and West Pokot that have lower HIV incidence rate but high TB burden. We attribute these exceptions to unsuccessful treatment critical to arresting TB re-infections and new infections. In terms of competitive exclusion, TB can exist in places where HIV is of low incidence

Although TB disproportionately affects persons living with HIV, most of the transmission is by persons without HIV, who typically remain transmissible for a longer period. Since delayed diagnosis influences the prolongation of infectiousness and effective treatment rapidly attenuates infectiousness (45,46), initiatives to reduce TB incidence in the general population can help prevent new infections among persons living with HIV.

The primary limitation of the study is using case notification data as a surrogate measure of the general population at risk. Case notifications are data from specific subpopulations who seek treatment and care from health facilities; these are geographically representative of nearby populations. Whereas this kind of data is not completely spatially random for the co-epidemic burden, it still captures the spatiotemporal patterns of incidence risk, which is the ultimate goal of this study.

Conclusion

Our study demonstrates the potential utility of case notification data in providing robust estimates for the broad spatiotemporal structure of the TB-HIV co-epidemic. The findings have shown that the high burden counties for TB-HIV co-infection are consistent with findings from previous work done on high burden counties for HIV. This suggests that the TB-HIV co-epidemic in Kenya is still at a critical point portending a dual endemic challenge for many years to come. Much as HIV is a serious challenge in the management of TB, the national response to TB-HIV coinfection promotes HIV testing among TB patients as a strategy to reduce TB transmission. However, the government of Kenya needs to combine surveillance systems for the TB and HIV National programs to optimize the TB-HIV coinfection case notification processes at all levels. With integrated case notification systems at the health facility levels, there will be complete data capture on co-infection incidences and outcomes. Integration of care for both TB and HIV using a single facility and single health provider in each county will enable proper monitoring of the co-infection trends, which will guide policy decisions on access to health care and relevant public health interventions. This will also ensure adequate resource allocation to cause a significant impact on the reduction of HIV burden amongst TB patients and TB burden amongst HIV patients

List of abbreviations

BYM Besag-York-Mollie

CI Confidence Interval

Ď mean deviance

DIC	Deviance Information Criterion
FEM	Fixed Effects Model
HIV	Human Immunodeficiency Virus
iCAR	intrinsic Conditional Autoregressive Model
INLA	Integrated Nested Laplace Approach
NLTP	National Tuberculosis, Leprosy and Lung Disease Program
pD	effective number of parameters
TB	Tuberculosis

Declarations

Ethics approval and consent to participate

This study used data with all participant identifiers removed. Ethical permission for use of the data in the present study was obtained from National Tuberculosis, Leprosy and Lung Disease Program (NLTP) - Kenya.

Consent for publication

Not applicable

Availability of data and material

The datasets used and/ or analyzed during the current study are available from the corresponding author on reasonable request.

Competing interests

The authors declare that they have no competing interests.

Funding

The authors would like to thank the African Union and Pan African University Institute of Basic Sciences Technology and Innovation (PAUISTI) for funding the study through VO's Ph.D. work.

Authors' contributions

VO conceived, designed the study and wrote the first draft of the manuscript. VO and TO analyzed data. HM contributed to data analysis. All authors contributed to reviewing literature, interpretation of the results and writing of the manuscript. All authors read and approved the final manuscript.

Acknowledgments

The authors sincerely thank the National Tuberculosis, Leprosy and Lung Cancer Program (NLTP) for providing the data used in this study. The authors acknowledge the help of Prof Gabriel Magoma for commenting on earlier drafts of the manuscript.

Author's information

[1]Department of Mathematical Sciences, Pan African University Institute of Basic Sciences Technology and Innovation, Nairobi, Kenya

[2]Epidemiology and Biostatistics Division, School of Public Health, University of the Witwatersrand, Johannesburg, South Africa

[3]School of Mathematics, Statistics & Computer Science, University of Kwa Zulu Natal, Pietermaritzburg, South Africa

References

1. Kumar A, Kumar AM V, Gupta D, Kanchar A, Mohammed S, Srinath S, et al. Global guidelines for treatment of tuberculosis among persons living with HIV: unresolved issues. Int J Tuberc Lung Dis. 2012 May;16(5):573–8.

2. Khan FA, Minion J, Pai M, Royce S, Burman W, Harries AD, et al. Treatment of active tuberculosis in HIV-coinfected patients: a systematic review and meta-analysis. Clin Infect Dis. 2010 May 1;50(9):1288–99.

3. Mayer KH, Hamilton CD. Synergistic Pandemics: Confronting the Global HIV and Tuberculosis Epidemics. Clin Infect Dis. 2010 May 15;50(s3):S67–70.

4. WHO. Global Tuberculosis Report 2016. World Health Organization; 2016. 214 p.

5. Nkhoma K, Ahmed A, Ali Z, Gikaara N, Sherr L, Harding R. Does being on TB treatment predict a higher burden of problems and concerns among HIV outpatients in Kenya? a cross-sectional self-report study. AIDS Care. 2018 Jun 20;30(sup2):28–32.

6. Whalen CC, Zalwango S, Chiunda A, Malone L, Eisenach K, Joloba M, et al. Secondary attack rate of tuberculosis in urban households in Kampala, Uganda. PLoS One. 2011 Feb 14;6(2):e16137.

7. Dheda K, Shean K, Zumla A, Badri M, Streicher EM, Page-Shipp L, et al. Early treatment outcomes and HIV status of patients with extensively drug-resistant tuberculosis in South Africa: a retrospective cohort study. Lancet. 2010 May 22;375(9728):1798–807.

8. Patel NR, Swan K, Li X, Tachado SD, Koziel H. Impaired M. tuberculosis-mediated apoptosis in alveolar macrophages from HIV+ persons: potential role of IL-10 and BCL-3. J Leukoc Biol. 2009 Jul;86(1):53–60.

9. Bell LCK, Noursadeghi M. Pathogenesis of HIV-1 and Mycobacterium tuberculosis co-infection. Nat Rev Microbiol. 2017 Nov 7;16(2):80–90.

10. Van-Rie A, Westreich D, Sanne I. Tuberculosis in patients receiving antiretroviral treatment: incidence, risk factors, and prevention strategies. J Acquir Immune Defic Syndr. 2011 Apr;56(4):349–55.

11. Gupta A, Wood R, Kaplan R, Bekker L-G, Lawn SD. Tuberculosis incidence rates during 8 years

of follow-up of an antiretroviral treatment cohort in South Africa: comparison with rates in the community. PLoS One. 2012;7(3):e34156.

12. Winter JR, Adamu AL, Gupta RK, Stagg HR, Delpech V, Abubakar I. Tuberculosis infection and disease in people living with HIV in countries with low tuberculosis incidence. Int J Tuberc Lung Dis. 2018 Jul 1;22(7):713–22.

13. Yuen CM, Weyenga HO, Kim AA, Malika T, Muttai H, Katana A, et al. Comparison of trends in tuberculosis incidence among adults living with HIV and adults without HIV--Kenya, 1998-2012. PLoS One. 2014;9(6):e99880.

14. Mbithi A, Gichangi A, Kim AA, Katana A, Weyenga H, Williamson J, et al. Tuberculosis and HIV at the national level in Kenya: results from the Second Kenya AIDS Indicator Survey. J Acquir Immune Defic Syndr. 2014 May 1;66(Suppl 1):S106–15.

15. WHO. Global tuberculosis report 2015. 20th ed. World Health Organization; 2015. 192 p.

16. Trinh QM, Nguyen HL, Nguyen VN, Nguyen TVA, Sintchenko V, Marais BJ. Tuberculosis and HIV co-infection-focus on the Asia-Pacific region. Int J Infect Dis. 2015 Mar;32:170–8.

17. Lin W-C, Lin H-H, Lee SS-J, Sy C-L, Wu K-S, Chen J-K, et al. Prevalence of latent tuberculosis infection in persons with and without human immunodeficiency virus infection using two interferon-gamma release assays and tuberculin skin test in a low human immunodeficiency virus prevalence, intermediate tuberculosis-b. J Microbiol Immunol Infect. 2016 Oct;49(5):729–36.

18. Karo B, Krause G, Hollo V, van der Werf MJ, Castell S, Hamouda O, et al. Impact of HIV infection on treatment outcome of tuberculosis in Europe. AIDS. 2016 Apr;30(7):1089–98.

19. Onyango DO, Yuen CM, Cain KP, Ngari F, Masini EO, Borgdorff MW. Reduction of HIV-associated excess mortality by antiretroviral treatment among tuberculosis patients in Kenya. Cameron DW, editor. PLoS One. 2017 Nov 16;12(11):e0188235.

20. Onyango DO, Yuen CM, Masini E, Borgdorff MW. Epidemiology of Pediatric Tuberculosis in

399 Kenya and Risk Factors for Mortality during Treatment: A National Retrospective Cohort Study. J
400 Pediatr. 2018 Oct;201:115–21.

401 21. Schrödle B, Held L. A Primer on Disease Mapping and Ecological Regression Using INLA.
402 Comput Stat. 2010;26(2):241–58.

403 22. Ugarte MD, Adin A, Goicoa T, Militino AF. On fitting spatio-temporal disease mapping models
404 using approximate Bayesian inference. Stat Methods Med Res. 2014;23(6):507–30.

405 23. Blangiardo M, Cameletti M, Baio G, Rue H. Spatial and spatio-temporal models with R-INLA.
406 Spat Spatiotemporal Epidemiol. 2013;4:33–49.

407 24. Bernardinelli L, Clayton D, Pascutto C, Montomoli C, Ghislandi M, Songini M. Bayesian analysis
408 of space - time variation in disease risk. Stat Med. 1995;14:2433–43.

409 25. HDR. Technical Note 3. 2015.

410 26. CRA. Creating a County Development Index to identify marginalized counties. Nairobi, Kenya;
411 2012. Report No.: 01.

412 27. Richardson S, Abellan JJ, Best N. Bayesian spatio-temporal analysis of joint patterns of male and
413 female lung cancer risks in Yorkshire (UK). Stat Methods Med Res. 2006;15(4):385–407.

414 28. WHO. TB burden estimates, notifications and treatment outcomes: For individual countries and
415 territories, WHO regions and the world. 2018.

416 29. Osei E, Der J, Owusu R, Kofie P, Axame WK. The burden of HIV on Tuberculosis patients in the
417 Volta region of Ghana from 2012 to 2015: implication for Tuberculosis control. BMC Infect Dis.
418 2017 Dec 19;17(1):504.

419 30. Tarekegne D, Jemal M, Atanaw T, Ebabu A, Endris M, Moges F, et al. Prevalence of human
420 immunodeficiency virus infection in a cohort of tuberculosis patients at Metema Hospital,
421 Northwest Ethiopia: a 3 years retrospective study. BMC Res Notes. 2016 Dec 29;9(1):192–8.

31. Sanchez M, Bartholomay P, Arakaki-Sanchez D, Enarson D, Bissell K, Barreira D, et al. Outcomes of TB treatment by HIV status in national recording systems in Brazil, 2003-2008. PLoS One. 2012;7(3):e33129.

32. Davy-Mendez T, Shiau R, Okada RC, Moss NJ, Huang S, Murgai N, et al. Combining surveillance systems to investigate local trends in tuberculosis-HIV co-infection. AIDS Care. 2019 Feb 7;1–8.

33. Sánchez MS, Lloyd-Smith JO, Williams BG, Porco TC, Ryan SJ, Borgdorff MW, et al. Incongruent HIV and tuberculosis co-dynamics in Kenya: Interacting epidemics monitor each other. Epidemics. 2009 Mar;1(1):14–20.

34. Manjareeka M, Nanda S. Prevalence of HIV infection among tuberculosis patients in Eastern India. J Infect Public Health. 2013 Oct;6(5):358–62.

35. van der Werf MJ, Ködmön C, Zucs P, Hollo V, Amato-Gauci AJ, Pharris A. Tuberculosis and HIV coinfection in Europe: looking at one reality from two angles. AIDS. 2016;30(18):2845–53.

36. Chanda-Kapata P, Kapata N, Klinkenberg E, Grobusch MP, Cobelens F. The prevalence of HIV among adults with pulmonary TB at a population level in Zambia. BMC Infect Dis. 2017;17(1):236.

37. Lee JY. Diagnosis and treatment of extrapulmonary tuberculosis. Tuberc Respir Dis (Seoul). 2015 Apr;78(2):47–55.

38. Magadi MA. Understanding the gender disparity in HIV infection across countries in sub-Saharan Africa: evidence from the Demographic and Health Surveys. Sociol Health Illn. 2011 May;33(4):522–39.

39. Sitienei J, Nyambati V, Borus P. The Epidemiology of Smear Positive Tuberculosis in Three TB/HIV High Burden Provinces of Kenya (2003–2009). Epidemiol Res Int. 2013;2013:1–7.

40. Sia D, Onadja Y, Nandi A, Foro A, Brewer T. What lies behind gender inequalities in HIV/AIDS

in sub-Saharan African countries: evidence from Kenya, Lesotho and Tanzania. Health Policy Plan. 2014 Oct;29(7):938–49.

41. Sia D, Onadja Y, Hajizadeh M, Heymann SJ, Brewer TF, Nandi A. What explains gender inequalities in HIV/AIDS prevalence in sub-Saharan Africa? Evidence from the demographic and health surveys. BMC Public Health. 2016 Dec 3;16(1):1136.

42. Horton KC, MacPherson P, Houben RMGJ, White RG, Corbett EL. Sex Differences in Tuberculosis Burden and Notifications in Low- and Middle-Income Countries: A Systematic Review and Meta-analysis. PLoS Med. 2016 Sep;13(9):e1002119.

43. MacNab YC. On Gaussian Markov Random Fields and Bayesian disease mapping. Lawson AB, editor. Stat Methods Med Res. 2011 Feb 14;20(1):49–68.

44. Cuadros DF, Li J, Branscum AJ, Akullian A, Jia P, Mziray EN, et al. Mapping the spatial variability of HIV infection in Sub-Saharan Africa: Effective information for localized HIV prevention and control. Sci Rep. 2017 Dec 22;7(1):9093.

45. Dye C, Glaziou P, Floyd K, Raviglione M. Prospects for Tuberculosis Elimination. Annu Rev Public Health. 2013 Mar 18;34(1):271–86.

46. Nardell E, Dharmadhikari A. Turning off the spigot: reducing drug-resistant tuberculosis transmission in resource-limited settings. Int J Tuberc Lung Dis. 2010 Oct;14(10):1233–43.

List of figure legends

Figure 1: Temporal trend of co-infection risk by gender

Figure 2: Spatial patterns of co-infection burden by gender

Figure 3: Temporal trend of co-infection by age-category

Figure 4: Spatial patterns of co-infection burden by age category

List of tables legends

Figures

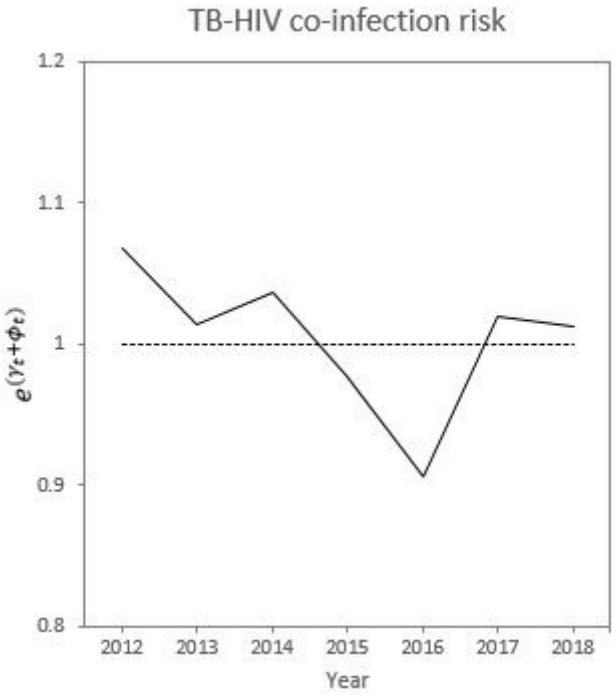

Figure 1

Temporal trend of co-infection risk in Kenya

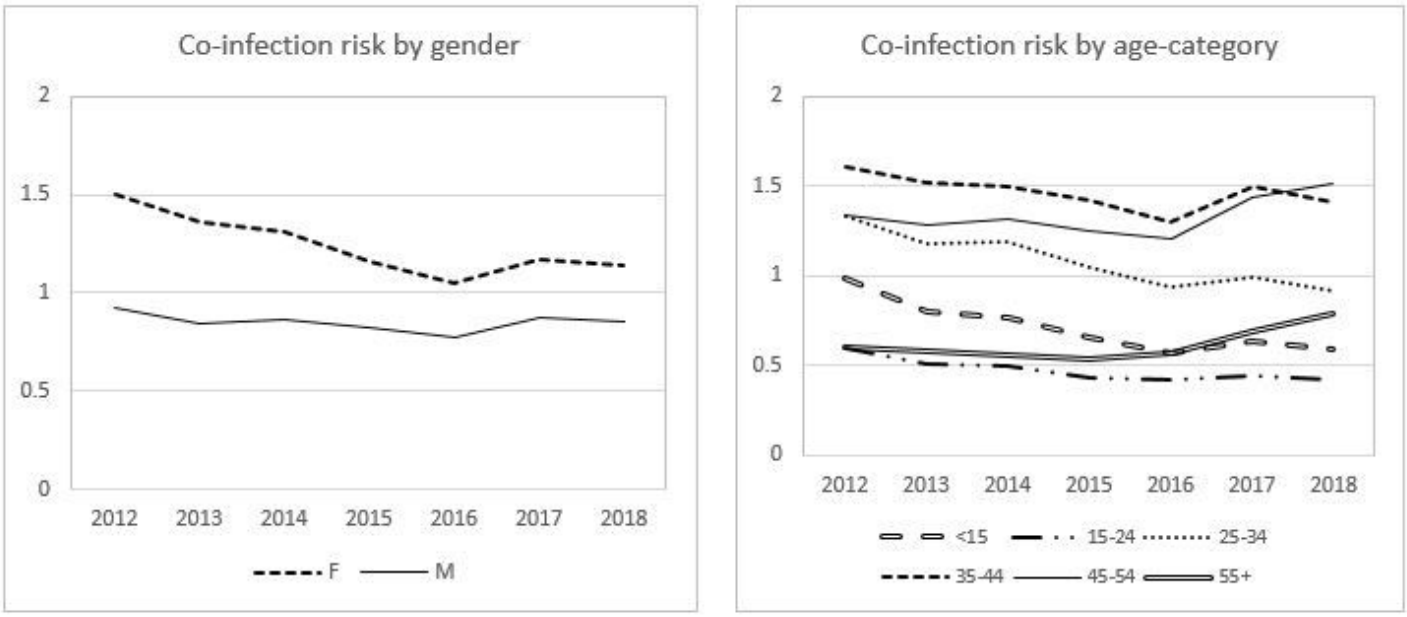

Figure 2

Temporal trend of co-infection risk by gender and age-category

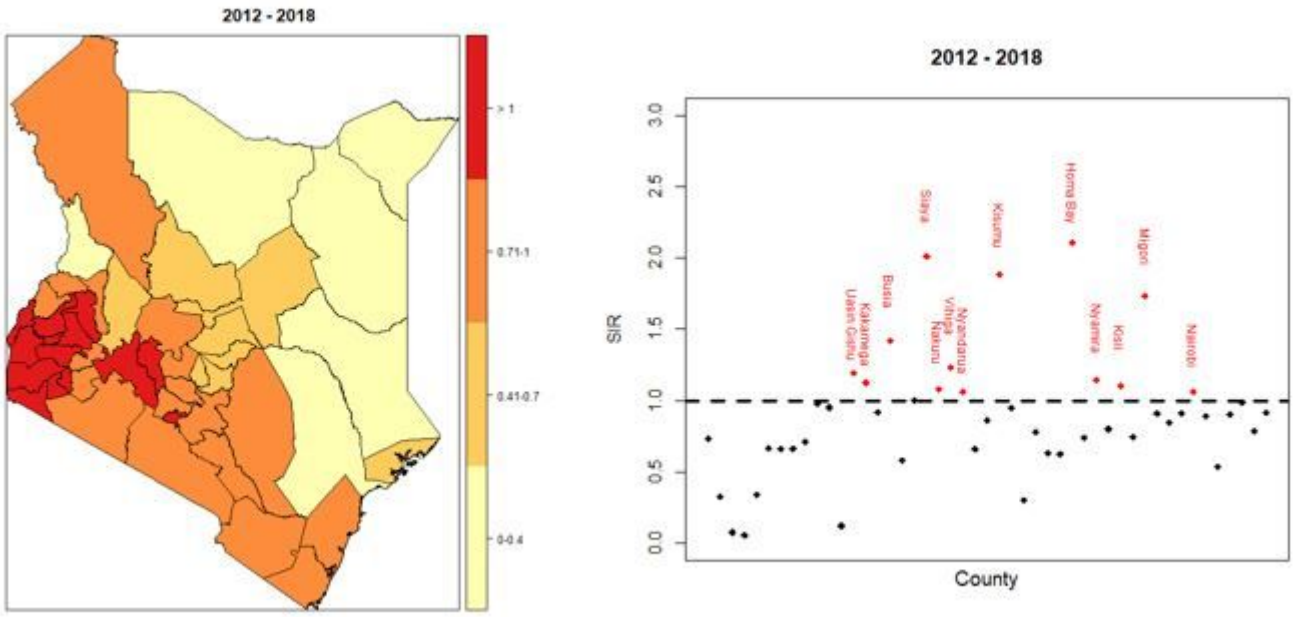

Figure 3

Spatial pattern of co-infection burden per County (2012 - 2018)

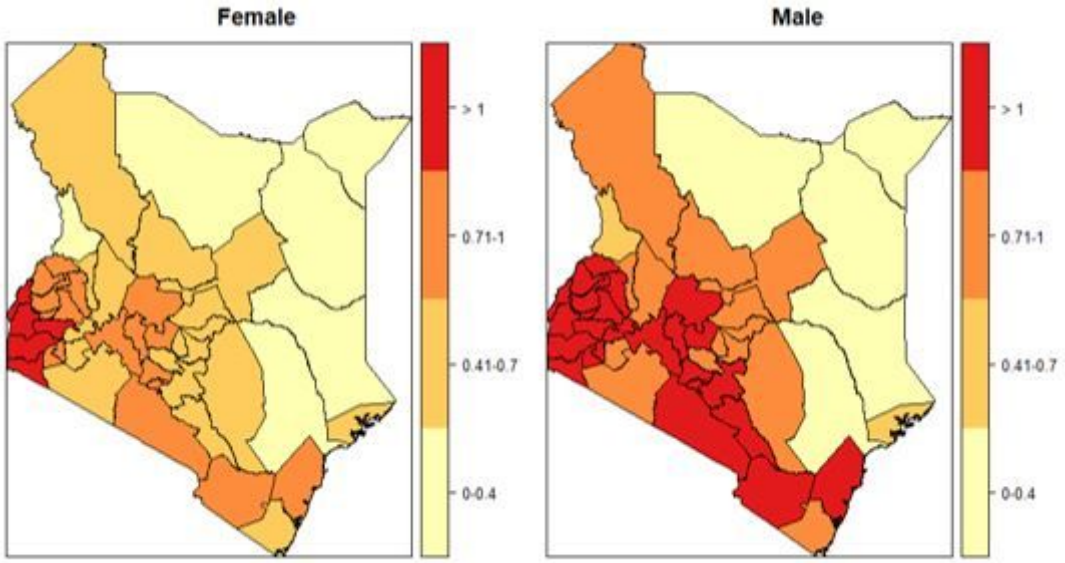

Figure 4

Spatial patterns of co-infection burden by gender

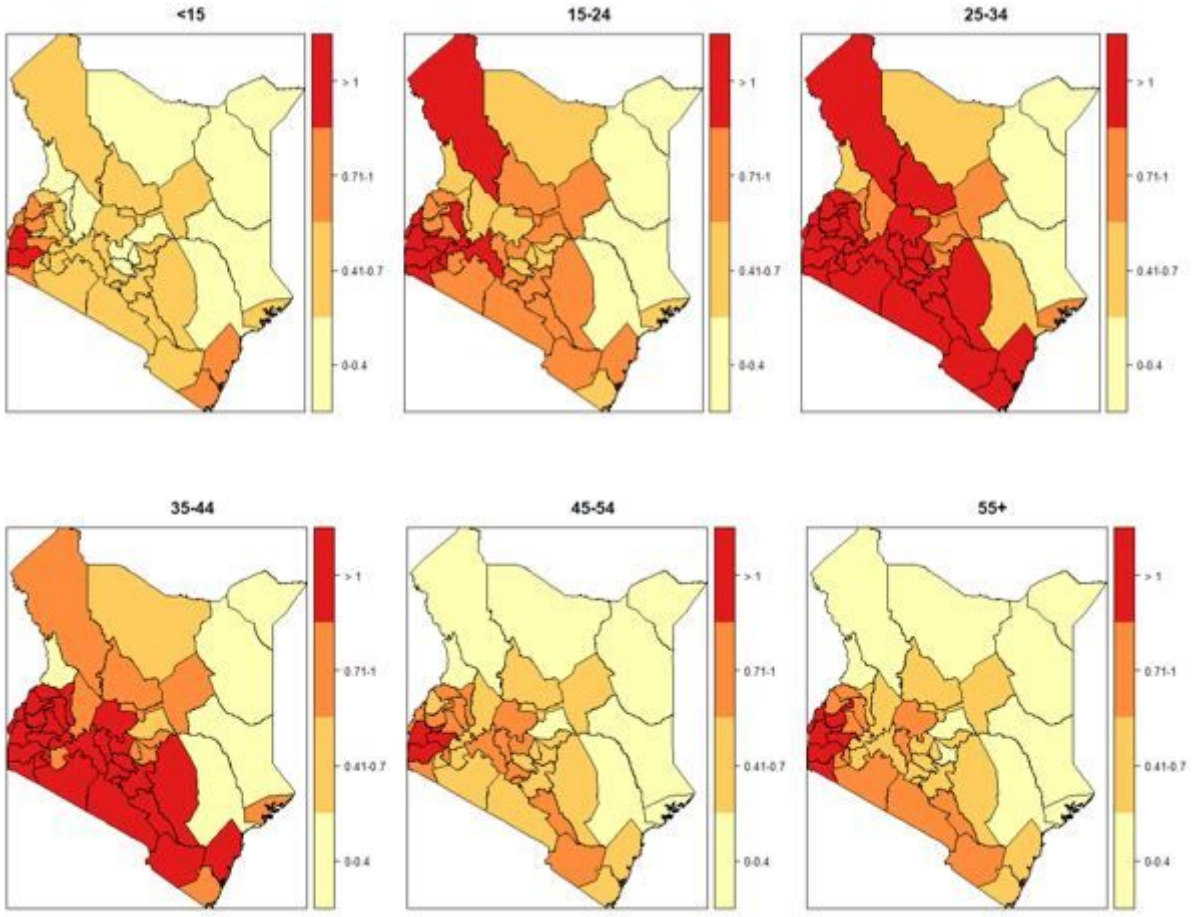

Figure 5

Spatial patterns of co-infection burden by age category

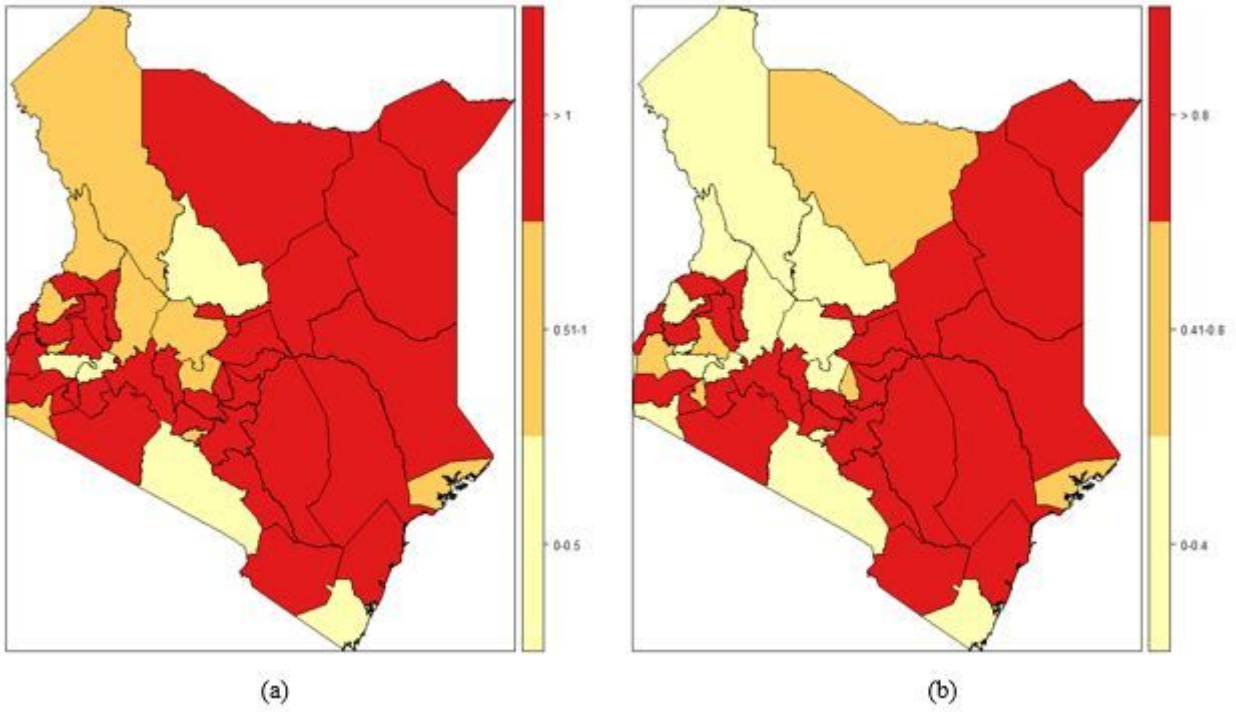

Figure 6

County-specific relative risks and posterior probabilities. (a) Spatial pattern of coinfection risk (b) Uncertainty for the spatial effect

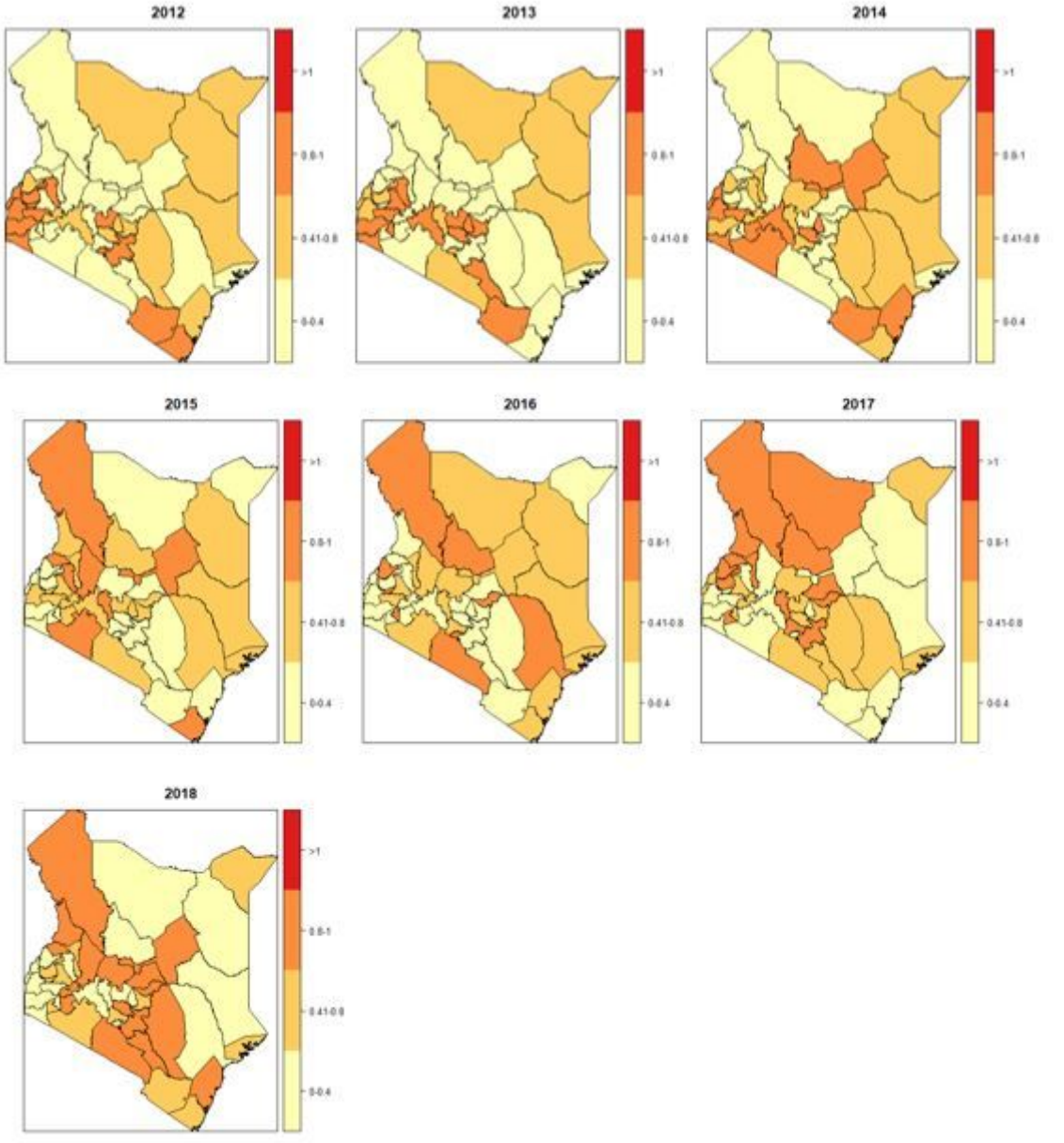

Figure 7

Posterior probabilities for the space-time interaction: 47 counties and 2012-2018 years